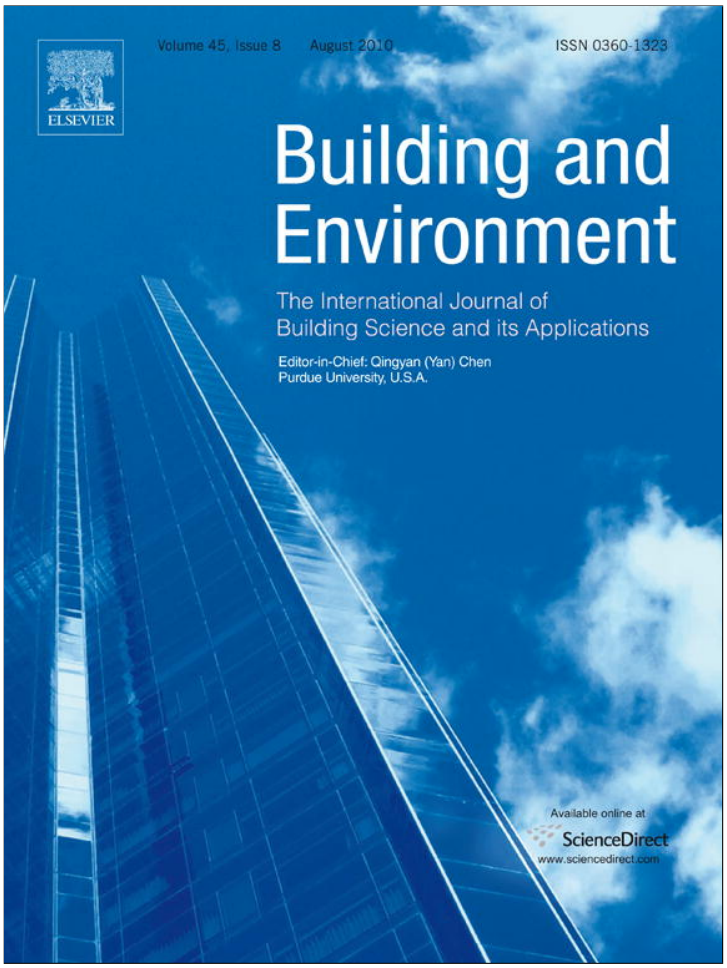

Building and Environment 45 (2010) 1880–1889

Contents lists available at ScienceDirect

Building and Environment

journal homepage: www.elsevier.com/locate/buildenv

A simple method for designation of urban ventilation corridors and its application to urban heat island analysis

Man Sing Wong, Janet E. Nichol*, Pui Hang To, Jingzhi Wang

Department of Land Surveying and Geo-Informatics, The Hong Kong Polytechnic University, Kowloon, Hong Kong

ARTICLE INFO

Article history:
Received 7 December 2009
Received in revised form
22 February 2010
Accepted 24 February 2010

Keywords:
Frontal area index
Geographic information systems
Remote sensing
Urban heat island
Ventilation path

ABSTRACT

This paper describes urban wind ventilation mapping, using the concept of "building frontal area index", and uses the Kowloon peninsula of Hong Kong as an example of a dense, sub-tropical urban environment where ventilation is critical for human health. The frontal area index is calculated for uniform 100 m grid cells, based on three dimensional buildings in each cell, for eight different wind directions. The frontal area index is then correlated with a land use map, and the results indicate that high density commercial and industrial areas with large building footprints had higher values than other urban land use types. Using the map of frontal area index, the main ventilation pathways across the urban area are located using least cost path analysis in a raster GIS. Field measurements of urban winds confirmed the significance and functionality of these modelled ventilation paths. Comparison of the pathways with a map of the urban heat island suggests that ventilation is a key parameter in mitigating heat island formation in the study area. Planning and environmental authorities may use the derived frontal area index and ventilation maps as objective measures of environmental quality within a city, especially when temperatures in the inner city are a major concern.

1. Introduction

The urban heat island (UHI) is defined as the temperature difference between urban and rural areas. As urban populations increase, many cities in both temperate [1–3] and tropical regions [4–9] are reporting significant heat island effects resulting from high building densities. Air flow between rural and urban areas is one of the parameters governing urban heat island formation and the build-up of pollution [3,10]. Low horizontal wind speeds are usually associated with high surface roughness, where energy is lost by vertical instability due to a high density of built structures [11]. The pressure differences along temperature gradients can also induce low-level breezes across the urban-rural boundary.

Most of the data included in wind and air quality studies are from ground level instruments. The gathering of data over large regions such as a city therefore, is a major challenge to these studies. Wind tunnel models provide another method for visualising the local wind direction and pollutant dispersion at large scales over a district. For example, Duijm [12] used the wind tunnel model in Lantau island, Hong Kong at a large scale (1:4000) over a small area, and Mfula et al. [13] tested a very large building model at 1:100 scale to identify pollution sources affecting buildings, based on wind and pollutant patterns at the surface. Although wind tunnel studies of urban ventilation can provide accurate wind models measured under constrained conditions, the small area coverage, high computer processing requirements and high operational cost often prohibit their usage. In recent years, a variety of numerical models have been developed for modelling air ventilation, such as the PSU/NCAR mesoscale model (known as MM5) and the computational fluid dynamics (CFD) model. The MM5 model works for mesoscale phenomena such as sea breezes and mountain–valley flows [14] with large area coverage at coarse resolution, while the CFD model simulates urban wind flows over smaller areas in greater detail. The CFD model is being widely used in engineering flow analysis, building and structural design, urban wind flow predictions [15], and air pollution dispersal modelling [16–18]. It comprises a set of physical models which attempt to closely match the real urban geometry and thus simulate the air flow around buildings and along streets. The CFD model is thus highly computer-intensive and generally inapplicable to large areas or whole cities. The only known exception to this is the use of a CFD model running on a supercomputer, which models temperature and air flow over a 5×5 km area of Tokyo [19]. Therefore, wind ventilation modelling at city scale, especially over densely urbanised regions with complex street and building structures is challenging.

* Corresponding author. Tel.: +852 27665952; fax: +852 23302994.
E-mail addresses: m.wong06@fulbrightmail.org (M.S. Wong), lsjanet@polyu.edu.hk (J.E. Nichol).

0360-1323/$ – see front matter © 2010 Elsevier Ltd. All rights reserved.
doi:10.1016/j.buildenv.2010.02.019

Now, geographic information systems (GIS) and remote sensing techniques can provide alternative solutions by adopting simplified assumptions and numerical approximations. Wind modelling for near surface conditions can be simplified mathematically by estimating roughness parameters from building structures. Several studies have modelled surface roughness using GIS and remote sensing techniques and several parameters have been suggested for calculation of surface roughness. These are zero-plane displacement height (z_d) and the roughness length (z_0) [20,21], plan area density (λ_p), frontal area index (λ_f) [22,23], average height weighted with frontal area (z_h), depth of the roughness sub-layer (z_r) [24,22] and the effective height (h_{eff}) [25] etc.

Among these urban morphological parameters, the "frontal area index" has been suggested as a good indicator of the roughness of the urban surface for mesoscale meteorological and urban dispersion models [22,23]. Frontal area index is the measurement of building walls facing the wind flow in a particular direction (frontal area per unit horizontal area) (Fig. 1). It has a strong relationship with surface roughness z_0, and is a function of the flow regime within urban street canyons [23]. Gál and Unger [26] calculated the frontal area index from lot area polygons in Szeged, Hungary for depicting the potential ventilation paths over the city. They suggested lot area polygons as the unit for frontal area calculation since the buildings in Hungary are individually separable and the density of built area in Szeged is far less (11%) than in the Kowloon peninsula of Hong Kong (71%). Although Gál and Unger [26] provided a thorough method for the depiction of ventilation paths using frontal area index and other parameters, the pathways were located mainly by visual inspection, and the results were not practically validated. More details of frontal area index will be given in Section 3.

The aims of this paper are (i) to demonstrate a simple automated method for deriving the frontal area index from three dimensional GIS building data, (ii) to demonstrate the use of the frontal area index map in least cost path (LCP) analysis to derive the frequency of occurrence of ventilation paths over the study area, and (iii) to identify the locations of major ventilation corridors and their relationships to urban heat island formation in the study area.

2. Study area

Hong Kong, a sub-tropical city with hot humid summers, suffers from the urban heat island effect caused by a high-rise, high density urban form, with population densities in the Kowloon peninsula exceeding 52,000 km^2 in some areas [9]. With temperature differences up to 9–10 °C between rural areas and the urban core [6,9], the Hong Kong population has recently shown great concern about the heat island effect. This is exacerbated by planning policies which allow building developers to maximise profits by blocking sea views resulting in the so-called "wall effect" around the coastline, and depriving inner areas of ventilation. The study area is the Kowloon peninsula in Hong Kong, which is 160 km^2 in extent and has a population over 2 million. It comprises mainly high density residential and commercial districts, with one large park (Kowloon Park) and a few small urban parks of less than 1 ha each. The topography is mainly flat, but at the northern edge, elevation rises to 300 m. Media reports suggest a strong belief by residents that the wall effect is a major cause of the urban heat island, by preventing cool sea breezes from reaching the inner city, and since Kowloon is a peninsula, this is a reasonable assumption. In planning for future urban renewal, data are needed to confirm and analyse the influence of ventilation on urban temperatures.

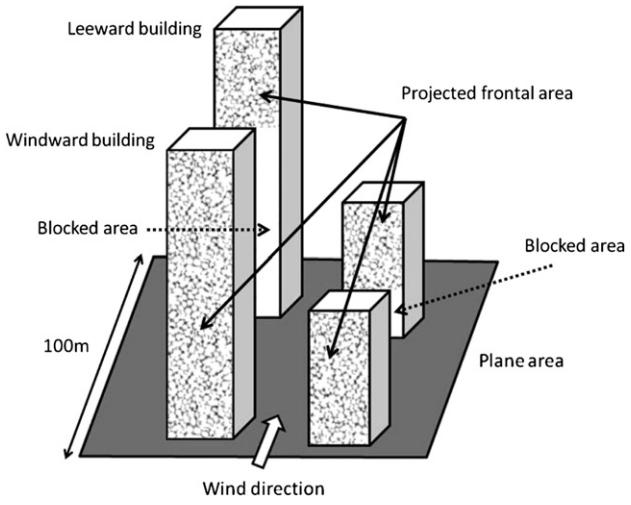

Fig. 1. Example of frontal area calculation.

3. Methods

3.1. Calculation of frontal area index

The frontal area index (λ_f) is calculated as the total area of building facets projected to plane normal facing the particular wind direction (and independent of the angle of the building facets), divided by the plane area (equation (1)) [22,23].

$$\lambda_f = A_{facets}/A_{plane} \quad (1)$$

where λ_f is the frontal area index, A_{facets} is the total area of building facets facing the wind direction, and A_{plane} is the plane area. Therefore, a λ_f of $\geq$1.0 means that wind is mostly blocked by buildings within a selected plane region (e.g. $A_{facets} \geq A_{plane}$), and a λ_f of ca. 0.5 means that wind is half blocked (e.g. $2 \times A_{factors} \approx A_{plane}$).

Burian et al. [23] used a similar approach for estimating the λ_f in Los Angeles. Digital data of building polygons at 1:5000 scale were obtained from the Hong Kong Lands Department. A program was written in ESRI® ArcGIS™ 9.2 software to estimate the total frontal area in the projected plane normal to the specific wind direction. In this study we modified Grimmond and Oke and Burian et al.'s [22,23] algorithm by eliminating the areas blocked by buildings upwind, from the blocked area on leeward buildings (Fig. 1). This program is first set up for a particular wind direction and it generates projected lines in the wind direction with a 5 m horizontal increment. If the projected lines hit the first facet and do not reach the second facet, only the frontal area of the first facet is calculated. This modification of the original method is important for irregular building groups, and can reduce the number of facets being calculated in computer memory. The calculated frontal areas are then re-grouped based on horizontal plane polygons (e.g. grid cell of 100 m $\times$ 100 m, which is the resolution of the study).

We used grid cells of 100 m $\times$ 100 m size to calculate the λ_f because the Hong Kong Planning Department [27] in Hong Kong found that a grid resolution of 100 m was compatible with all variables used for determining dynamic potential and thermal load contributions in an urban climatic study. Also, since Nichol and Wong [28] show that a resolution of 200 m corresponds to intra-urban differences in air temperature between different land cover types, then a resolution of 100 m is more than adequate. Thus, our study calculated λ_f at 100 m grid resolution over the Kowloon peninsula (approx. 11 km by 7 km) for eight different wind directions (north, northeast, east, southeast, south, southwest, west, and northwest).

Since the most densely built areas are devoid of vegetation, and elsewhere street planting is severely restricted by lack of space [29], urban vegetation is small and fragmented. Since urban vegetation has a small frontal area compared to buildings, trees are not considered in the λ_f calculation. In addition, since the urban topography is mainly flat, terrain is also not considered.

3.2. Frontal area index in different land use types

In Hong Kong, as in most cities, different land use types support different building structures and characteristics. For example high-rise buildings in residential areas have over 50 floors compared with only 20–30 floors in commercial districts, and industrial buildings have larger footprint, and 20–50 storeys. Therefore, it was expected that these areas would have different λ_f properties. This study used a digital land use map at 10 m resolution from the Hong Kong Planning Department for analysing the relationship between λ_f and different land uses.

3.3. Relationship between frontal area index and environmental parameters

Five environmental parameters, namely heat island intensity (HII), aerosol optical thickness (AOT) air quality derived from a satellite image, vegetation cover (NDVI) derived from a Landsat image, building density (BD), and building height (BH) were mapped over the study area. HII represents the air temperature difference between the urban pixels and a rural climatic station at the image time, derived from a previous study [9], and the Normalized Difference Vegetation Index (NDVI) is a measure of vegetation amount. Table 1 describes the sources of the parameters, their units, and their resolutions. The parameters HII and AOT represent typical distributions of aerosols and temperature over the urban area. Although the data were derived from a single image time, both HII and AOT are closely related to the urban structure and activities, and are observed by the researchers to be spatially stable at different seasons of the year. All maps were then regressed against the derived λ_f map and the correlations were tabulated (see Section 4.2).

3.4. Least cost path analysis

In order to predict the likely air flow corridors based on the premise that wind across a city follows the path of least resistance, least cost path (LCP) analysis was undertaken to designate these pathways across the city. LCP analysis identifies the path of least resistance across a cost surface from a starting point to an ending point. The pathways represent routes with a high probability of strong ventilation and a high degree of connectivity between starting and ending points. This study adopted the approach of allocating variable weightings to the frontal area index value of each pixel, e.g. the higher λ_f, the higher the friction value. The friction values represent the percentage of obstruction of wind ventilation or air flow for that 100 m pixel. By varying the λ_f classes and/or the friction weightings, it is possible to designate a few major pathways or many minor pathways. For example, this study adopted variable weightings in order to generate many different paths.

Firstly, the λ_f map was imported to IDRISI v.14.02 (Clark Labs., Worcester, MA, USA). The λ_f pixel values were reclassified into five classes and each class was given a friction value according to the degree of wind obstruction, with higher friction values given to large frontal area values. The friction values were set to increase gradually with higher λ_f values (Table 2). This assumes that air is most obstructed in areas with high λ_f values, but is not completely obstructed if the cost-distance of using an alternative path outweighs the cost of a cell's λ_f value. Secondly, starting points for the air flows were designated. For example, fifty points were spaced evenly along the east coast of the Kowloon peninsula representing starting points for the easterly wind travelling across the peninsula from east to west. The friction surface was then created by the IDRISI COST module which computed the cost surfaces for the fifty starting points. Thirdly, fifty ending points located along the west coast of Kowloon peninsula were input to the PATHWAY module [30] for generating LCPs from the starting points to these ending points. A total of 2500 and 5186 LCPs represent eastward and northeasterly winds respectively, from the combinations of multiple starting and ending points. Due to the large number of starting and ending points, the LCPs overlapped each other in many places, i.e. many grid cells have many LCPs running through them. The occurrence frequencies were calculated by counting the overlaid LCP pathways for each cell. Thus, grid cells with high occurrence frequencies are associated with low frontal area index values represented by low friction values. These cells are likely to have stronger air flow and better ventilation than those with few, or no paths passing through them. All these processes were implemented by customised scripts in IDRISI, and the results are shown in Section 4.4.

4. Results

4.1. Map of λ_f

Fig. 2 shows the distribution of λ_f which represents the average frontal area index values calculated for all eight directions. An average value of $\lambda_f = 0.25$ is observed over the whole study area, with significantly high λ_f values near the west coast of the peninsula, caused by newly developed high-rise buildings (>300 m high) creating the so-called "wall effect" described in Section 2. These high-rise buildings are also shown by our study to have a significant relationship with the UHI (Section 2).

4.2. Relationship between λ_f and different land use types

Table 3 shows λ_f as a function of different land use types. The industrial and commercial areas have significantly higher λ_f (0.324 and 0.305) than other areas. The residential class has moderate to high λ_f (~0.254) values, and public transportation and warehouses

Table 1
Data sources.

Parameters	Unit	Source	Source resolution
HII	°C	ASTER image on 31 Jan 2007	10 m after emissivity correction [8]
AOT	–	CHRIS/PROBA satellite images on 18 Dec 2005 and 06 Feb 2007	90 m
NDVI	–	Landsat image on 17 Sep 2001	30 m
BD	–	LIC (GIS) 1:1000 data	Tertiary Planning Unit
BH	Meter	LIC (GIS) 1:1000 data	Rasterised to 10 m, Tertiary Planning Unit

Table 2
Friction values allocated to different classes of λ_f.

Allocated friction value	λ_f
20	<0.2
40	0.2–0.4
60	0.4–0.6
80	0.6–0.8
100	>0.8

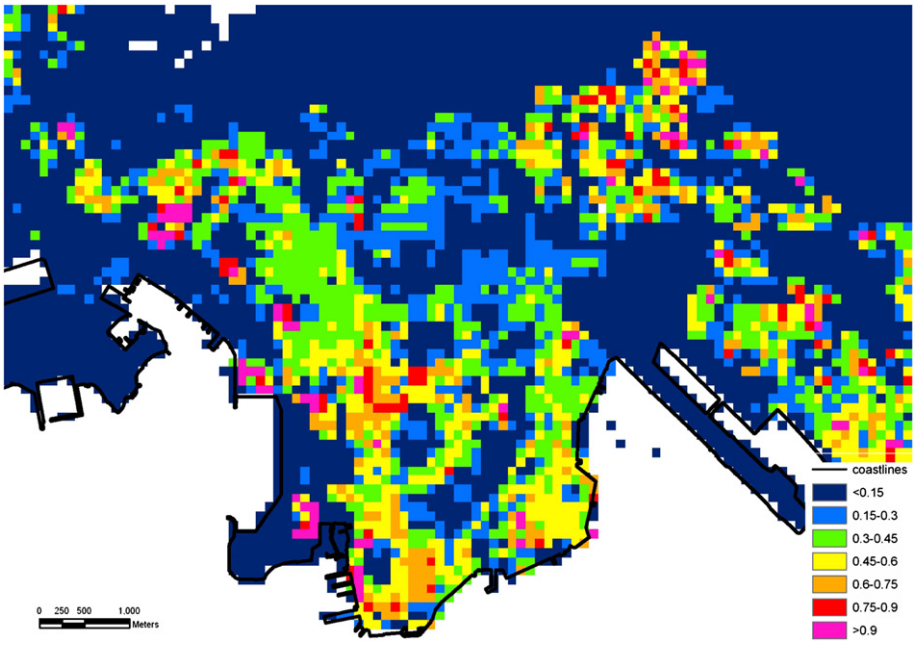

Fig. 2. Map of frontal area index.

have lower λ_f ($\sim$0.15) values. Our findings indicate a direct relationship between the frontal area index and the building characteristics, with higher λ_f always associated with wider and taller buildings (e.g. industrial and commercial districts). Burian et al. [23] found that the λ_f in residential, commercial, industrial and public transportation districts in Los Angeles, were 0.176, 0.246, 0.095, 0.011 respectively based on the irregular grid cells ($>$10000 m^2) of the street network. Grimmond and Oke [22] studied the λ_f over small areas immediately surrounding meteorological stations in North America, finding the highest λ_f in the city center in Vancouver, Canada (0.3) and in suburban residential areas in Arcadia, United States (0.33). Since their methods of calculating λ_f included the frontal areas for every facet, their values would be expected to be much higher than ours. The fact that our values are higher, testifies to the extremely high density built environment of the Kowloon peninsula, and the problems of human comfort from which it suffers, compared with these temperate zone cities.

4.3. Correlations between λ_f and environmental parameters

The relationships between λ_f and environmental parameters were analysed at regional scale, within 68 Tertiary Planning Units (TPU), which sub-divide the city into a number of street blocks and village clusters, and are regarded as basic socioeconomic units (Table 4). All parameters at regional scale have higher correlations than at pixel scale and most of the parameters are significant at the 1% confidence level. Of the individual parameters, HII obtained the highest correlation ($r = 0.757$), and both BD and BH also have strong correlations with λ_f, since λ_f represents the plane and vertical aspects of building geometry. Vegetation cover (NDVI) shows strong negative correlation with λ_f. Only moderate correlation was observed with AOT ($r = 0.315$, $r = 0.251$ at regional and pixel levels respectively), but this may be due to the difficulty of mapping aerosols accurately at high resolution from satellite images.

Table 3
Frontal area index in different land use types.

Land use type	Averaged λ_f with eight directions
Private residential	0.267
Public residential	0.241
Commercial/business & offices	0.305
Industrial	0.324
Warehouse & storage	0.155
Rural settlements	0.056
Vegetation	0.075
Public transportation	0.15
Vacant development land	0.191

4.4. Ventilation paths

The eastward and northeastward maps of λ_f gave somewhat similar results (Fig. 3a and b), but they differ in the distribution of path frequencies (Fig. 3c and d; the cross and triangle symbols represent the starting and ending points of the LCPs). A total of 2500 and 5186 pathways were created from easterly and northeasterly directions respectively. The distribution of the occurrence frequency of LCPs shows that the areas with high probability of easterly wind ventilation paths are mostly located on

i. Boundary Street (A in Fig. 3c). This route traverses across low-rise low-density residential areas in which high-rise building was restricted due to the airport flight path. This street marks the boundary between Kowloon in the south which was ceded to the United Kingdom in 1860, and the New Territories which were leased to the United Kingdom in 1898. The occurrence frequency of LCPs along this route is greater than

Table 4
Correlations between λ_f and six environmental parameters at TPU district and pixel levels, and the number of samples.

Parameter	Correlation (r)	
	Regional level	Pixel level
HII	0.757	0.452
AOT	0.315	0.251
NDVI	−0.674	−0.449
BD	0.603	0.522
BH	0.527	0.383
n (Number of samples)	68	6504

30%, i.e. 750 out of the 2500 east–west paths are generated along Boundary Street.

ii. Argyle Street and Cherry Street (B in Fig. 3c). This is the shortest route, but is a wide four-lane dual-carriageway which connects the old airport in the east to the west coast. This route provides a strategic air corridor in the east–west direction since it bisects the most densely built part of MongKok. The occurrence frequency of LCPs along this route is greater than 18% (i.e. 450/2500).

iii. Ho Man Tin Hill road, King's Park road and Gascoigne road (C in Fig. 3c). This route traverses a large patch of urban vegetation, low-density residential development with fragmented trees, and dense commercial areas at the southern end. The occurrence frequency of LCPs along this route is ca. 16% (i.e. 400/2500) which is the lowest frequency among the three main paths.

These three routes have occurrence frequencies greater than 16%, and flow directions are from the east toward reclaimed land areas on the west coast. For the northeasterly paths generated, the corridor with the greatest frequency of paths (28%) was located on

iv. Princess Margaret road, Chatham road, Hong Chong road and Salisbury road (D in Fig. 3d). This route is located along the direction of the roads as they join end to end, and passes through low-rise residential areas, urban parks, a university

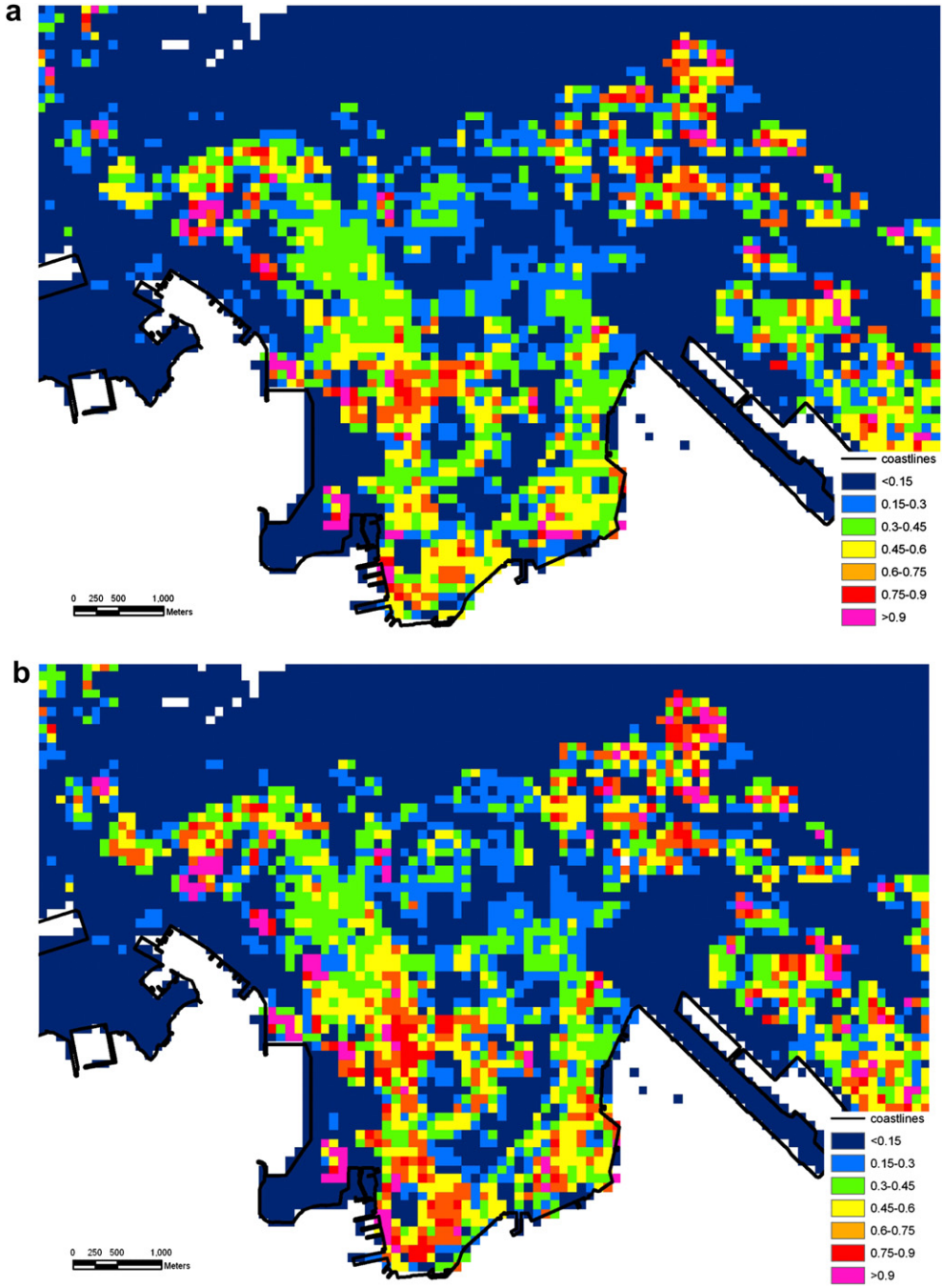

Fig. 3. a. Frontal area index map in east–west direction; b. Frontal area index map in northeast–southwest direction; c. Occurrence frequency of ventilation paths in east–west direction (total number of paths is 2500); d. Occurrence frequency of ventilation paths in northeast–southwest direction (total number of paths is 5186).

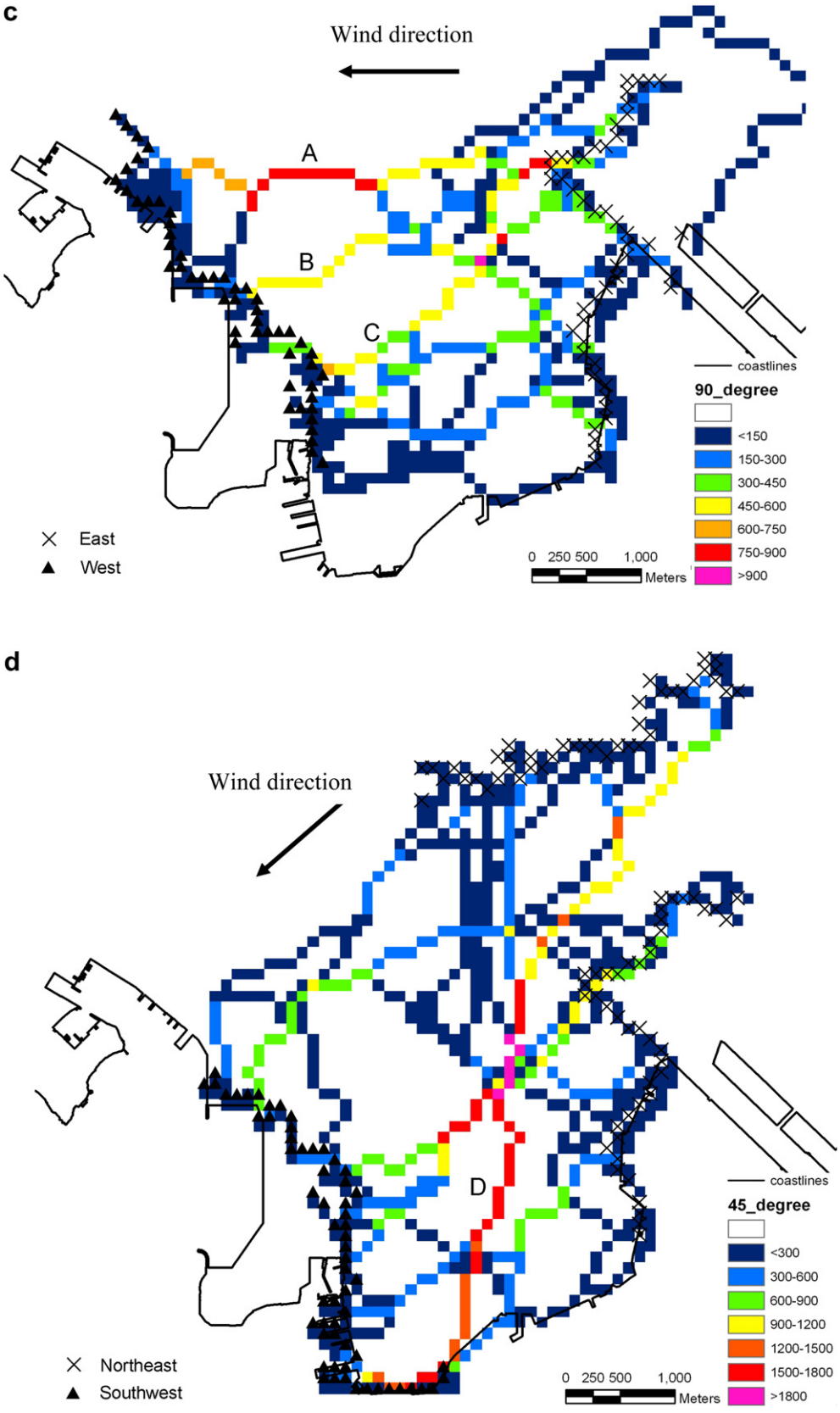

Fig. 3. (*continued*).

campus, a commercial district and harbor walkway. This route is represented by occurrence frequency greater than 28% (1500 out of 5186 paths).

These four pathways generated were considered to have a high probability of stronger and more frequent air movement than other areas. Since the easterly and northeasterly winds account for 66% of all the winds in Hong Kong, only these two directions were calculated in this study.

These maps of ventilation paths facilitate the visualisation of wind ventilation and show the specific locations in the city e.g. those in red and purple colours, which have the highest frequency of occurrence of paths are potential air flow corridors. (For interpretation of the references to colour in text, the reader is referred to the

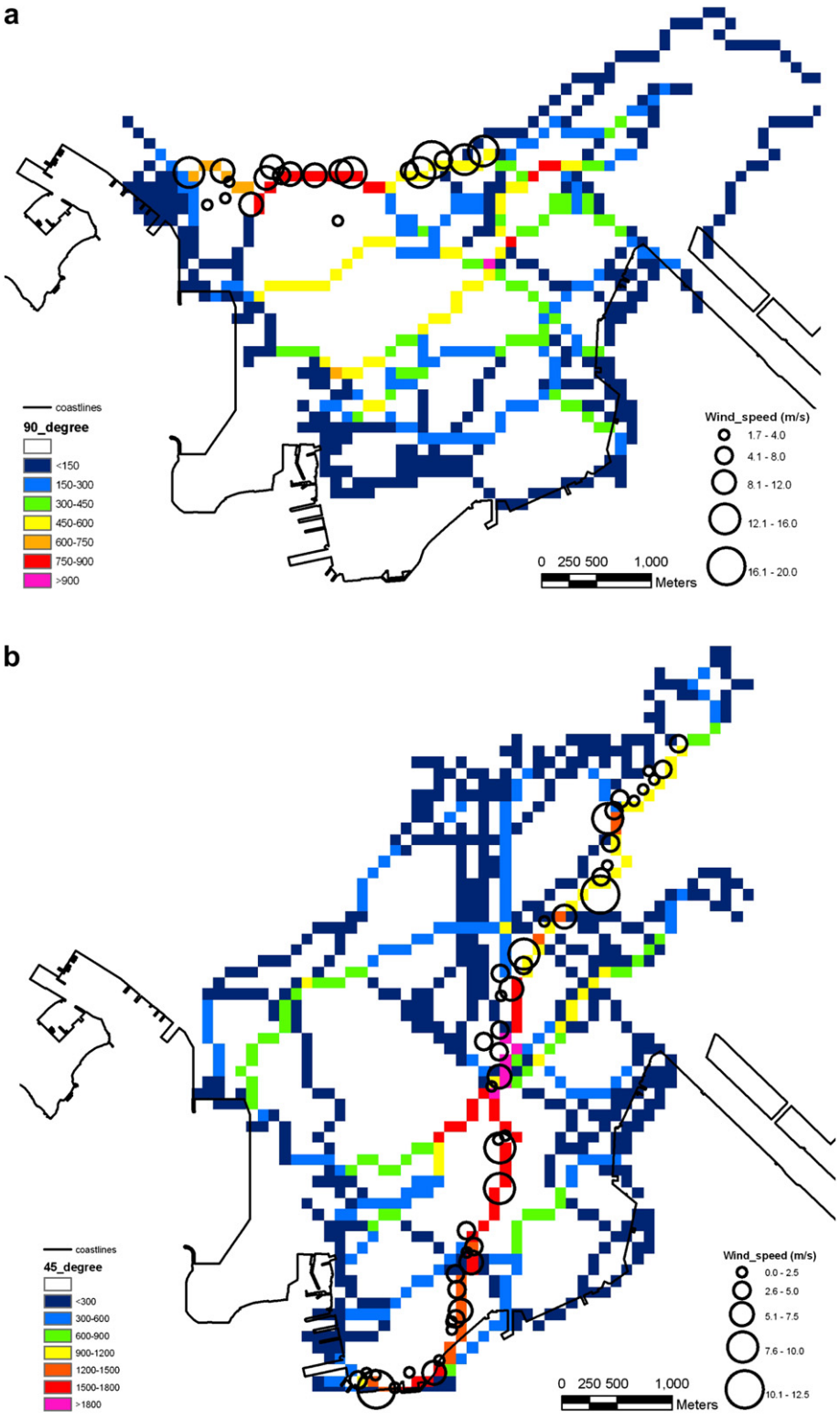

Fig. 4. Occurrence frequency of ventilation paths overlaid with field measurements in a. east–west direction, b. northeast–southwest direction.

web version of this article.) This enables better understanding of air ventilation at local scale, as well as over the whole urban area, whereas previous studies using the concept of λ_f have been conducted at local scale, for small city districts. When the whole urban area is considered, identification of the ventilation corridors by visual inspection from a building plan and/or a map of frontal area index alone would be impossible due to the complexity of the building and street network. For example, in our study, because the four pathways traverse the whole urban area, each path is influenced by a large number of buildings (average of 436) and comprises many changes of direction (average of 24) along a route, and furthermore, LCP analysis considers distance values as well as λ_f in the computation. On the other hand, the study by Gál and Unger ([26], op cit) describe a visual (non-automated) method for identifying the ventilation paths, which appear unable to traverse the central urban areas, and only general ventilation paths are drawn.

4.5. Validation strategy

In order to investigate the significance and functionality of the ventilation paths, fieldwork was undertaken on 09 Oct 2009, 13 Oct 2009, 15 Oct 2009, when winds were at 45, 90, and 45°, which are representative of the dominant east and northeasterly winds throughout the year. A slow walk was undertaken along the differing sections of the routes A and D, recording the wind speed and GPS locations along the routes. The wind speeds were measured four times for each section, resulting in 22 and 48 readings from routes A and D respectively, and the results were averaged. These two routes were chosen because of the high occurrence frequencies of ventilation paths. Fig. 4 shows the field measurements overlaid onto the ventilation paths, and the dot sizes represent the wind speeds along the route. Along route A, average and maximum wind speeds of 9.3 ms^{-1} and 17.8 ms^{-1} were observed respectively. However, wind speeds off the pathway were much lower (ca. 2.3 ms^{-1}), and more similar to the background wind speed of 2 ms^{-1} for Kowloon recorded by the Hong Kong Observatory at the time. About 55% of the field readings with wind speed above 9.1 ms^{-1} fall in route A (which has 24% of all paths generated). This identifies route A as a key connecting corridor along which air flows in the dominant wind direction, from the eastern to the western parts of the Kowloon peninsula. Along route D, the average and maximum wind speeds were lower than for route A, namely 3.5 ms^{-1} and 12.4 ms^{-1} respectively. But again the speeds along the route were much higher than that off the route (ca. 1.1 ms^{-1}) as well as higher than the background wind speed of 0.65 ms^{-1}. This validation study confirmed that analysis of the frequency of occurrence of ventilation paths does indeed indicate relevant ventilation corridors over the city, since the highest field measured wind speeds corresponded to the corridor with the highest frequency of paths from the LCP analysis i.e. route A with 30% of all paths generated, and wind speeds off the paths were much lower.

Fig. 5 shows the designated ventilation paths overlaid onto the image of HII which has a 10 m resolution. Red and purple areas indicate the core regions of the urban heat island, having large temperature differences from the rural areas. All four paths cross these core areas at the shortest distance, especially route B, which

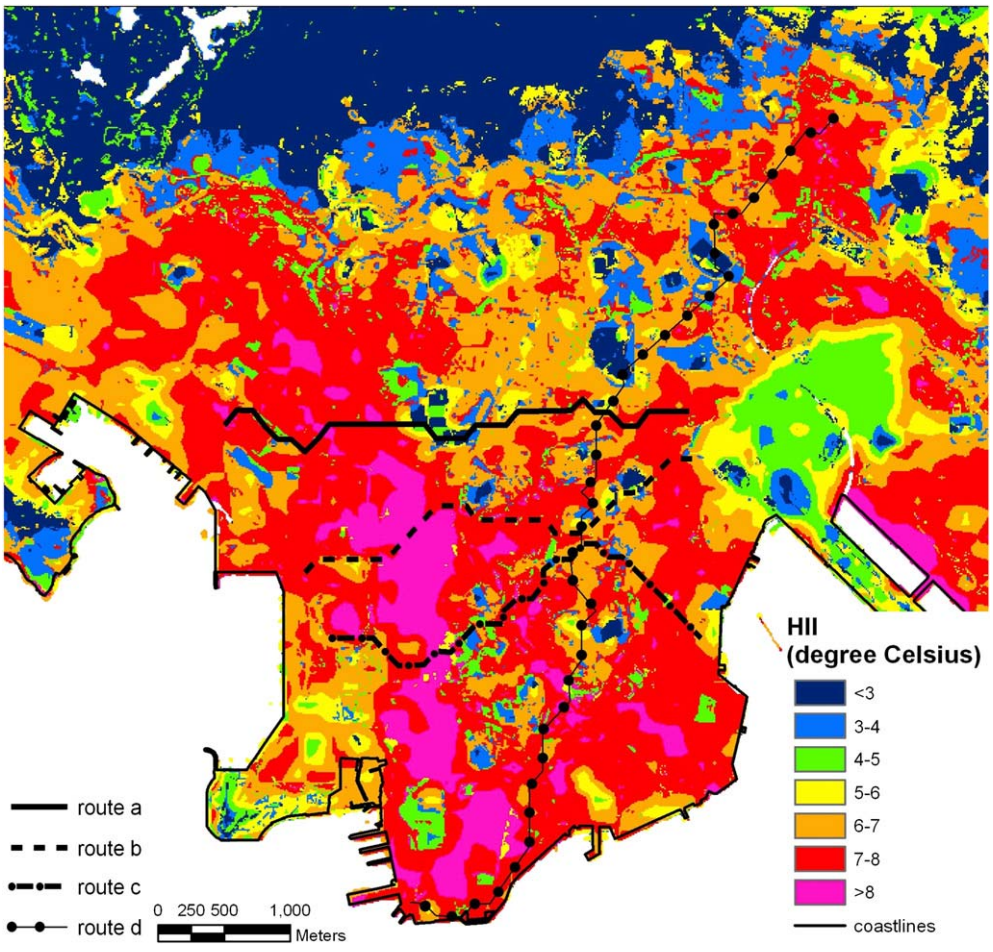

Fig. 5. Designated ventilation paths overlaid on heat island intensity image at 10 m resolution.

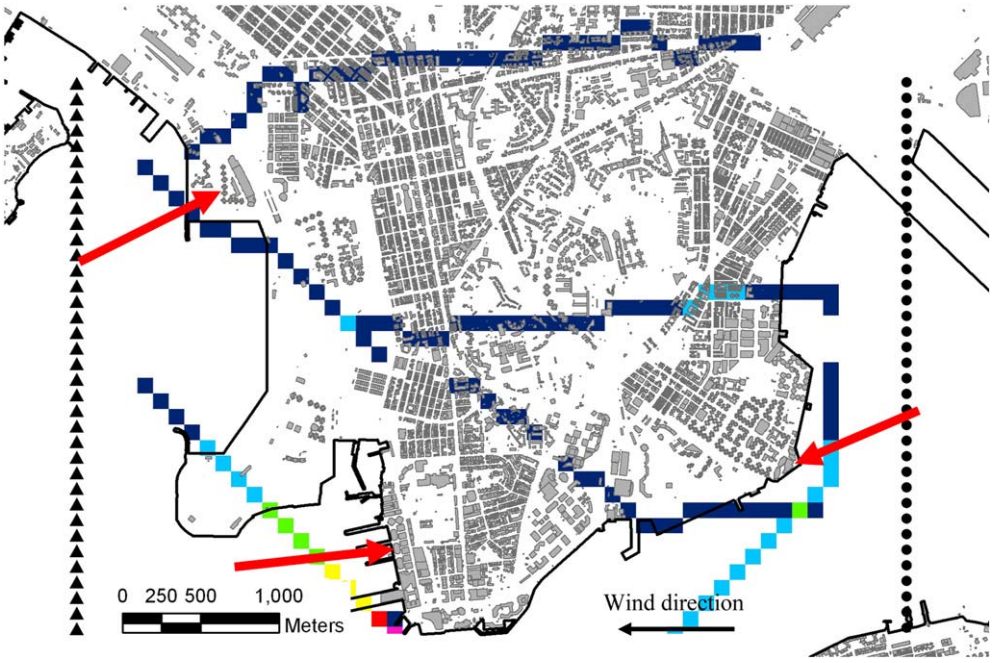

Fig. 6. Ventilation paths located using offshore starting and ending points to test the "wall effect" along coastlines. Red arrows indicate main locations of "wall effects" due to high-rise building parallel to the coast, referred to in media reports. Colour legend as for Fig. 3c. (For interpretation of the references to colour in this figure legend, the reader is referred to the web version of this article.)

passes through the core heat island region of MongKok (the highest populated district in the world). Route D also passes through green open spaces with low HII, avoiding the core built areas with high HII values. These observations suggest that adequate ventilation is indeed a key requirement for controlling the temperatures in inner areas of densely built, high-rise cities such as Kowloon. Indeed it may also be suggested that without the observed ventilation corridors, the existing core heat island areas would expand and amalgamate to form a larger and more compact entity.

Fig. 6 shows ventilation corridors located by LCP analysis using starting and ending points offshore, in order to test the "wall effect" due to high-rise buildings along the coast, which has been a cause of concern to the Hong Kong public. It is obvious that the paths avoid, and have to navigate around the two coastlines with major wall effect buildings (red arrowed areas). A comparison with Fig. 5 indicates high HII values immediately or more generally inland of these highly built coastlines, comprising heat island core areas.

5. Conclusion

This paper investigates urban ventilation pathways using the frontal area index model over a densely built urban area, the Kowloon peninsula of Hong Kong. We calculated the frontal area index based on three dimensional building data and expressed this as a function of land use type. Most of the frontal area indices as a function of land use type were found to be greater than those computed for other studies elsewhere, and commercial and industrial areas were found to have significantly high values because these areas are high-rise in Hong Kong. The environmental parameters heat island intensity (HII), building density (BD), and building height (BH) were found to have significant positive correlations with frontal area index, while vegetation cover (NDVI) had a significant negative relationship. These suggest that the frontal area index presented herein is a useful parameter in mesoscale meteorological studies and can contribute to heat island analysis.

To evaluate ventilation corridors at city scale, LCP analysis was performed. However, whereas LCP analysis usually operates with a single or few pathways, this study overlaid all LCP paths to derive maps of frequency of occurrence of LCPs. Four major ventilation corridors travelling from easterly and northeasterly directions were identified from these maps. The corridors, routes A, B, C and D accounted for 30%, 18%, 16% and 28% respectively, of all least cost paths, and they travel from easterly and northeasterly directions respectively. Wind speeds were measured in the field to evaluate the relevance of the models, and these compare well with the frequencies of the modelled pathways.

In densely urbanised Hong Kong, the ventilation corridors of 100 m width used in this study may not appear to provide viable connecting corridors at street scale, but are sufficient for city scale modelling, as demonstrated by the analysis of the urban heat island. However, the model of frontal area index can be adapted for any grid resolution depending on the morphology of any particular city. This study offers a simple and low cost method to investigate the ventilation conditions of any city at a highly detailed level. City planners and environmental authorities may use the derived maps for pinpointing the key buildings restricting air flow to the urban core. Thus the living environment in future urban renewal projects may easily be improved by a simple shift in location and orientation of buildings, while maintaining the same plot ratios, and the creation of ventilation corridors will not decrease ventilation elsewhere. The λ_f values calculated for this study did not account for terrain elevation, since the study area was mainly flat. This could easily be achieved by converting the grid to a DEM, and allocating a DEM value weighting to the $\lambda_f$values in each cell. Furthermore, if the main objective of designating ventilation paths was to maximise human comfort rather than for heat island analysis, then ground level is more important than the tops of tall buildings, and a lower weight should be allocated to high level building facets. Other future improvements to the model may include consideration of the type of surface, since winds traversing a vegetated surface have a greater cooling capacity than those traversing impervious surfaces.

Acknowledgments

The authors would like to acknowledge the Hong Kong Planning Department for land use and Tertiary Planning Unit data and the Lands Department for building GIS databases. This project was funded by PolyU SURF project 1-ZV4V.

References

[1] Baker L, Brazel A, Selover N, Martin C, McIntyre N, Steiner F, et al. Urbanization and warming of Phoenix (Arizona, USA): impacts, feedbacks and mitigation. Urban Ecosystems 2003;6:183–203.
[2] Hawkins T, Brazel A, Stefanov W, Bigler W, Saffell E. The role of rural variability in urban heat island determination for Phoenix, Arizona. Journal of Applied Meteorology 2004;43(3):476–86.
[3] Oke TR. The energetic basis of the urban heat island. Quarterly Journal of the Royal Meteorological Society 1982;108:1–24.
[4] González JE, Luvall JC, Rickman DL, Comarazamy D, Picón AJ. Urban heat island identification and climatological anlaysis in a coastal, tropical city: San Juan, Puerto Rico. In: Weng Q, Quattrochi DA, editors. Urban remote sensing. Florida: CRC Press; 2007. p. 223–52.
[5] Jusuf SK, Wong NH, Hagen E, Anggoro R, Hong Y. The influence of land use on the urban heat island in Singapore. Habitat International 2007;31:232–42.
[6] Fung WY, Lam KS, Nichol JE, Wong MS. Heat island study – satellite derived air temperature. Journal of Climate and Applied Meteorology 2009;48(4):863–72.
[7] Nichol JE. High resolution surface temperature patterns related to urban morphology in a tropical city: a satellite-based study. Journal of Applied Meteorology 1996;35:135–46.
[8] Nichol JE. Remote sensing of urban heat islands by day and night. Photogrammetric Engineering and Remote Sensing 2005;71(5):613–21.
[9] Nichol JE, Fung WY, Lam KS, Wong MS. Urban heat island diagnosis using ASTER satellite images and 'in situ' air temperature. Atmospheric Research 2009;94(2):276–84.
[10] Haeger-Eugensson M, Holmer B. Advection caused by the urban heat island circulation as a regulating factor on the nocturnal urban heat island. International Journal of Climatology 1999;19:975–88.
[11] Oke TR. Boundary layer climates. London and New York: Routledge; 1987.
[12] Duijm NJ. Dispersion over complex terrain: wind-tunnel modelling and analysis techniques. Atmospheric Environment 1996;30(16):2839–52.
[13] Mfula AM, Kukadia V, Griffiths RF, Hall DJ. Wind tunnel modelling of urban building exposure to outdoor pollution. Atmospheric Environment 2005;39(15):2737–45.
[14] Dudhia J, Gill D, Manning K, Wang W, Bruyere C. PSU/NCAR mesoscale modeling system tutorial class notes and user's guide: MM5 modeling system version 3. NCAR; 2003.
[15] Baik JJ, Kim JJ. A numerical study of flow and pollutant dispersion characteristics in urban street canyons. Journal of Applied Meteorology 1999;38:1576–89.
[16] Blocken B, Carmeliet J, Stathopoulos T. CFD evaluation of the wind speed conditions in passages between buildings – effect of wall-function roughness modifications on the atmospheric boundary layer flow. Journal of Wind Engineering and Industrial Aerodynamics 2007;95(9–11):941–62.
[17] Huber AH, Tang W, Flowe A, Bell B, Kuehlert K, Schwarz W. Development and applications of CFD simulations in support of air quality studies involving buildings. In: Proceedings of 13th joint conference on the applications of air pollution meteorology with the Air & Waste Management Association. Vancouver, British Columbia, Canada; August 23–27 2004.
[18] Kondo H, Asahi K, Tomizuka T, Suzuki M. Numerical analysis of diffusion around a suspended expressway by a multi-scale CFD model. Atmospheric Environment 2006;40:2852–9.
[19] Ashie Y, Tokairin T, Kono T, Takahashi K. Numerical simulation of urban heat island in a ten-km square area of central Tokyo. In: Annual report of the Earth Simulator Center; 2007. p. 83–87.
[20] Lettau H. Note on aerodynamic roughness-parameter estimation on the basis of roughness-element description. Journal of Applied Meteorology 1969;8:828–32.
[21] Counihan J. Adiabatic atmospheric boundary layers: a review and analysis of data from the period 1880–1972. Atmospheric Environment 1975;9:871–905.
[22] Grimmond CSB, Oke TR. Aerodynamic properties of urban areas derived from analysis of surface form. Journal of Applied Meteorology 1999;34:1262–92.
[23] Burian SJ, Brown MJ, Linger SP. Morphological analysis using 3D building databases. LA-UR-02-0781. Los Angeles, CA: Los Alamos National Laboratory; 2002. 36–42.
[24] Bottema M. Urban roughness modelling in relation to pollutant dispersion. Atmospheric Environment 1997;31:3059–75.
[25] Matzarakis A, Mayer H. Mapping of urban air paths for planning in Munchen, 16. Wissenschaftlichte Berichte Institut for Meteorologie und Klimaforschung, The University of Karlsruhe; 1992. 13–22.
[26] Gál T, Unger J. Detection of ventilation paths using high-resolution roughness parameter mapping in a large urban area. Building and Environment 2009;44:198–206.
[27] The Hong Kong Planning Department. Urban Climatic Map and Standards for Wind Environment – Feasibility Study; 2009.
[28] Nichol JE, Wong MS. Spatial variability of air temperature over a city in a winter night. International Journal of Remote Sensing 2008;29(24):7213–23.
[29] Jim CY. Impacts of intensive urbanisation on trees in Hong Kong. Environmental Conservation 2004;25(2):146–59.
[30] Eastman R. IDRISI Andes tutorial. Worcester, USA: Clark Labs; 2006.